Effects of deep wet etching in HF/HNO_3 and KOH solutions on the laser damage resistance and surface quality of fused silica optics at 351 nm

Mathilde Pfiffer, Philippe Cormont, Evelyne Fargin, Bruno Bousquet, Marc Dussauze, Sébastien Lambert, Jérôme Neauport

Research Article | Vol. 25, No. 5 | 6 Mar 2017 | OPTICS EXPRESS 4607
Optics EXPRESS

Effects of deep wet etching in HF/HNO_3 and KOH solutions on the laser damage resistance and surface quality of fused silica optics at 351 nm

MATHILDE PFIFFER,[1,*] PHILIPPE CORMONT,[1] EVELYNE FARGIN,[2] BRUNO BOUSQUET,[3] MARC DUSSAUZE,[4] SÉBASTIEN LAMBERT,[5] AND JÉRÔME NÉAUPORT[1]

[1]*Commissariat à l'Energie Atomique et aux Energies Alternatives, Centre d'Etudes Scientifiques et Techniques d'Aquitaine, BP2, 33114 Le Barp, France*
[2]*Institut de Chimie de la Matière Condensée de Bordeaux, 33608 Pessac, France*
[3]*Centre Lasers Intenses et Applications, UMR 5107 CNRS, Université de Bordeaux, CEA, 33405 Talence, France*
[4]*Institut des Sciences Moléculaires, UMR 5255 CNRS, 33405 Talence, France*
[5]*Commissariat à l'Energie Atomique et aux Energies Alternatives, Le Ripault, BP16, 37260 Monts, France*
[*]*mathilde.pfiffer@cea.fr*

Abstract: We investigate the interest of deep wet etching with HF/HNO_3 or KOH solutions as a final step after polishing to improve fused silica optics laser damage resistance at the wavelength of 351 nm. This comparison is carried out on scratches engineered on high damage threshold polished fused silica optics. We evidence that both KOH and HF/HNO_3 solutions are efficient to passivate scratches and thus improve their damage threshold up to the level of the polished surface. The effect of these wet etchings on surface roughness and aspect is also studied. We show that KOH solution exhibit better overall surface quality that HF/HNO_3 solution in the tested conditions. Given the safety difficulties associated with the processing with HF, KOH solution appears as a pertinent alternative to HF deep wet etching.

OCIS codes: (140.3330) Laser damage; (220.4610) Optical fabrication.

References and links

1. J. Neauport, L. Lamaignere, H. Bercegol, F. Pilon, and J. C. Birolleau, "Polishing-induced contamination of fused silica optics and laser induced damage density at 351 nm," Opt. Express **13**(25), 10163–10171 (2005).
2. D. W. Camp, M. R. Kozlowski, L. M. Sheehan, M. Nichols, M. Dovik, R. Raether, and I. Thomas, "Subsurface damage and polishing compound affect the 355-nm laser damage threshold of fused silica surfaces," Proc. SPIE **3244**, 356–364 (1998).
3. A. Salleo, F. Génin, J. Yoshiyama, C. Stolz, and M. R. Kozlowski, "Laser-induced damage of fused silica at 355nm initiated at scratches," Proc. SPIE **3244**, 341–347 (1998).
4. T. Suratwala, L. Wong, P. Miller, M. D. Feit, J. Menapace, R. Steele, P. Davis, and D. Walmer, "Sub-surface mechanical damage distribution during grinding of fused silica," J. Non-Cryst. Solids **352**(52-54), 5601–5617 (2006).
5. D. Liao, X. Chen, C. Tang, R. Xie, and Z. Zhang, "Characteristics of hydrolyzed layer and contamination on fused silica induced during polishing," Ceram. Int. **40**(3), 4479–4483 (2014).
6. T. Suratwala, W. Steele, L. Wong, M. Feit, P. Miller, R. Dylla-Spears, N. Shen, and R. Desjardin, "Chemistry and formation of the Beilby layer during polishing of fused silica glass," J. Am. Ceram. Soc. **98**(8), 2395–2402 (2015).
7. Z. Wang, L. Wang, W. Peng, Y. Cao, J. Yang, L. Tang, and S. Li, "Origin and distribution of redeposition layer in polished fused silica," Opt. Eng. **54**(8), 085102 (2015).
8. X. Gao, G. Feng, L. Zhai, and Z. Shouhuan, "Effect of subsurface impurities of fused silica on laser-induced damage probability," Opt. Eng. **53**(2), 026101 (2014).
9. M. D. Feit, J. Campbell, D. Faux, F. Y. Genin, M. R. Kozlowski, A. M. Rubenchik, R. Riddle, A. Salleo, and J. Yoshiyama, "Modeling of laser-induced surface cracks in silica at 355-nm," Proc. SPIE **3244**, 350–355 (1998).
10. F. Y. Génin, A. Salleo, T. V. Pistor, and L. L. Chase, "Role of light intensification by cracks in optical breakdown on surfaces," J. Opt. Soc. Am. A **18**(10), 2607–2616 (2001).

#281375 https://doi.org/10.1364/OE.25.004607
Journal © 2017 Received 23 Nov 2016; revised 22 Jan 2017; accepted 26 Jan 2017; published 21 Feb 2017

Optics EXPRESS

11. M. Feit and A. Rubenchik, "Influence of subsurface cracks on laser induced surface damage," Proc. SPIE **5273**, 264 (2003).
12. H. Bercegol, P. Grua, D. Hebert, and J. P. Morreeuw, "Progress in the understanding of fracture related laser damage of fused silica," Proc. SPIE **6720**, 672003 (2007).
13. P. E. Miller, J. D. Bude, T. I. Suratwala, N. Shen, T. A. Laurence, W. A. Steele, J. Menapace, M. D. Feit, and L. L. Wong, "Fracture-induced subbandgap absorption as a precursor to optical damage on fused silica surfaces," Opt. Lett. **35**(16), 2702–2704 (2010).
14. C. Zhang, M. Xu, and C. Wang, "Light intensification effect of trailing indent crack in fused silica subsurface," Sci. China Phys. Mech. Astron. **58**(3), 1–6 (2015).
15. J. Menapace, B. Penetrante, D. Golini, A. Slomba, P. E. Miller, T. Parham, M. Nichols, and J. Peterson, "Combined advanced finishing and UV-laser conditioning for producing UV-damage-resistant fused silica optics," Proc. SPIE **4679**, 56–68 (2002).
16. R. Catrin, J. Neauport, D. Taroux, P. Cormont, C. Maunier, and S. Lambert, "Magnetorheological finishing for removing surface and subsurface defects of fused silica optics," Opt. Eng. **53**(9), 092010 (2014).
17. L. Wong, T. Suratwala, M. D. Feit, P. E. Miller, and R. Steele, "The effect of HF/NH_4F etching on the morphology of surface fractures on fused silica," J. Non-Cryst. Solids **355**(13), 797–810 (2009).
18. C. L. Battersby, L. M. Sheehan, and M. R. Kozlowski, "Effects of wet etch processing on laser-induced damage of fused silica surfaces," Proc. SPIE **3578**, 446–455 (1998).
19. T. I. Suratwala, P. E. Miller, J. D. Bude, W. A. Steele, N. Shen, M. V. Monticelli, M. D. Feit, T. A. Laurence, M. A. Norton, C. W. Carr, and L. L. Wong, "HF-based etching processes for improving laser damage resistance of fused silica optical surfaces," J. Am. Ceram. Soc. **94**(2), 416–428 (2011).
20. X. Jiang, Y. Liu, H. Rao, and S. Fu, "Improve the laser damage resistance of fused silica by wet surface cleaning and optimized HF etch process," Proc. SPIE **8786**, 87860Q (2013).
21. H. Ye, Y. Li, Z. Yuan, J. Wang, Q. Xu, and W. Yang, "Improving UV laser damage threshold of fused silica optics by wet chemical etching technique," Proc. SPIE **9532**, 953221 (2015).
22. S. Tso and J. Pask, "Reaction of glasses with hydrofluoric acid solution," J. Am. Ceram. Soc. **65**(7), 360–362 (1982).
23. G. A. C. M. Spierings, "Wet chemical etching of silicate glasses in hydrofluoric acid based solutions," J. Mater. Sci. **28**(23), 6261–6273 (1993).
24. D. Knotter, "Etching mechanism of vitreous silicon dioxide in HF-based solutions," J. Am. Chem. Soc. **122**(18), 4345–4351 (2000).
25. W. Wang, P. Lu, L. Han, C. Zhang, C. Yang, R. Su, and J. Chen, "Diffusion behavior of ammonium group and its interaction mechanisms with intrinsic defects in fused silica," Appl. Phys., A Mater. Sci. Process. **929**, 7 (2016).
26. D. Kendall and R. Shoultz, *Handbook of Microlithography, Micromachining, and Microfabrication vol. 2* (P. Rai-Choudhury, 1997), p72.
27. S. Kiyama, S. Matsuo, S. Hashimoto, and Y. Morihira, "Examination of etching agent and etching mechanism on femtosecond laser microfabrication of channels inside vitreous silica substrates," J. Phys. Chem. **113**, 11560–11566 (2009).
28. J. Neauport, J. Destribats, C. Maunier, C. Ambard, P. Cormont, B. Pintault, and O. Rondeau, "Loose abrasive slurries for optical glass lapping," Appl. Opt. **49**(30), 5736–5745 (2010).
29. S. E. de système optiques SESO, "Procédé de polissage d'au moins une surface d'un pièce à base de silicium," French Patent EP1066926A1 (2001).
30. P. Belleville, S. Lambert, M. Pfiffer, and P. Cormont, "Procédé pour améliorer la tenue au flux laser d'un composant optique," French Patent 1658944, (September 23, 2016).
31. International Standard, Nos. 21254–1–21254–4 (2011).
32. L. Jensen, M. Mrohs, M. Gyamfi, H. Mädebach, and D. Ristau, "Higher certainty of the laser-induced damage threshold test with a redistributing data treatment," Rev. Sci. Instrum. **86**(10), 103106 (2015).
33. J. Wang, Y. Li, Z. Yuan, H. Ye, R. Xie, X. Chen, and Q. Xu, "Producing fused silica optics with high UV-damage resistance to nanosecond pulsed lasers," Proc. SPIE **9532**, 95320H (2015).
34. M. Pfiffer, J. L. Longuet, C. Labrugère, E. Fargin, B. Bousquet, M. Dussauze, S. Lambert, P. Cormont, and J. Neauport, "Characterization of the polishing-induced contamination of fused silica optics," J. Am. Ceram. Soc., doc ID 14448 (published 15 September 2016, in press).
35. J. Xu, X. Xu, C. Wei, W. Gao, M. Yang, J. Shao, and S. Liu, "The effect of deep HF etching on the surface quality and figure of fused silica optics," Proc. SPIE **9575**, 95750P (2015).

1. Introduction

High power Inertial Confinement Fusion (ICF) laser systems, such as the National Ignition Facility (NIF, USA), the Laser MegaJoule (LMJ, France) and the SG series Laser Facility (SG-III, China), use fused silica optics as final optics operating at 351 nm. The life time of these optical components is reduced by laser damage which occurs under UV illumination and fluence in the 5-20 J/cm^2 range for nanosecond pulse duration.

Optics EXPRESS

Pollutants from the polishing fluid and defects such as surface scratches, digs and sub-surface damage (SSD) are main precursors of laser damage [1–3]. Experimental studies explained phenomena which are responsible of subsurface and surface damage creation [4] and impurities penetration [5–7] during the polishing process. Numerical studies completed the experimental works to understand and predict the influence of these precursors on the laser induced damage threshold (LIDT). For example, Gao *et al.* [8] proposed a thermal model based on the heating of inclusions to a critical temperature in order to evaluate the influence of various impurities on the LIDT. Researches about the influence of scratches and SSD revealed that these defects reduce the laser damage resistance because of electromagnetic field intensification and enhanced absorption due to surface features and possible local absorbers [9–14]. With these highlights, the polishing process has been optimized to reduce the amount of surface and subsurface defects. For example, investigations about the magnetorheological finishing (MRF) provided evidence that this polishing technique was able to remove surface and subsurface defects and so improved LIDT of fused silica optics operating in UV light when combined with a small wet chemical etching [15,16]. At this step, laser damage performance of surface was considerably improved up to the level needed for ICF laser facilities and became limited mainly by surface defects such as scratches and digs which thus had to be passivated.

Wet chemical etching was investigated on fused silica optics for this purpose. Wet etching is a chemical reaction between a reactant and fused silica which dissolves the top layer of the optical components. Therefore pollutants embedded in the polishing layer are removed and surface topography is changed. Wong *et al.* [17] focused on scratches profiles and developed a model to understand how these profiles change as a function of the amount of material removal. Etching effects on main laser damage precursors significantly enhance laser damage resistance [18–21]. HF based solutions are mainly used to etch fused silica [22–24]. HF based solution removes silica from the surface with the reaction [19]:

$$SiO_{2\,(solid)} + 3\,HF_2^-{}_{(aq)} + H^+_{(aq)} \rightarrow SiF_6^{2-}{}_{(aq)} + 2\,H_2O_{(aq)}\,.$$

Optics for the NIF and the SG series Laser facilities are usually treated with a solution composed of HF and NH_4F which is named Buffered Oxyde Etch (BOE). With this chemical solution, the ammonium group (NH_4) is responsible for the generation of $(NH_4)_2SiF_6$ precipitates [19] and can also diffuse in silica reacting with structural defects as Frenkel defects and dangling bond defects [25]. Unfortunately, these parasitical phenomena could limit the LIDT enhancement because the ammonium group could absorb the laser energy and trigger laser damage. Consequently, the BOE etching needs to be optimized by the addition of an ultrasonic agitation. This agitation is not necessary for an etching with a solution composed of HF and HNO_3 or HF only.

Microfabrication and microlithography investigated the potassium hydroxide (KOH) capacities as a fused silica etchant [26,27]. One potential advantage of a basic solution is that it is far easier to handle from a safety point of view than an acid HF solution. However, to the best of our knowledge, basic solutions have not been used up to now to fabricate high damage threshold UV optics. In this case, the chemical reaction is:

$$Si(OH)_4 + OH^- \leftrightarrow Si(OH)_3\,O^- + H_2O$$

Kendall and Shoultz [26] gave an empirical relation for the etch rate R over a wide range of both temperature and KOH concentration:

$$R = 2.2\times10^9 W\left(1.5\times10^{-4}W^{2.15}\right)\exp-\left(0.795+6\times10^{-6}W^{2.5}\right)/kT\,,$$

where R is the etch rate in micrometers per hour, W is the wt% of KOH in water, k is Boltzmann's constant of 8.617×10^{-5} eV/K, and T is the temperature in Kelvin.

The main goal of this study was to compare the ability of an acid and a basic etching on to improve surface defect (scratches) damage threshold i.e. to passivate scratches. Moreover, as

Optics EXPRESS

etching is a final step of the manufacturing process, surface quality and optical properties must be kept above a quality level compatible with the use on a high power laser facility. Therefore we also compare the effect of these wet etching solutions on surface quality, a point that was rarely detailed in the literature.

To reach these goals we prepared fused silica substrates with polished surfaces and scratched surfaces, and then etched the samples with a HF-based solution or an OH-based solution. Sample preparation and etching processes are detailed in paragraph 2.1. We observed surface quality of etched polished surface with a defects mapping system and we measured roughness with an interferometer and an atomic force microscope. The surface chemical properties were studied with a surface free energy measurement and XPS analysis of the superficial bonds. Results of these surface characterizations are presented in the section 3.1. Characterizations of the scratches and more particularly their laser damage probabilities are detailed in paragraph 3.2. Finally, we discuss and conclude (sections 4 and 5) about the performances obtained with a basic etching in comparison with HF etching on fused silica optics.

2. Experimental setup

2.1 Samples preparation and etching processes

The six fused silica samples (Corning 7980, 50 mm diameter x 5 mm thick) used for this study were manufactured with an optimized grinding process which reduces the subsurface damage [28] followed by a pre-polishing and a super polishing [29]. Therefore they had a high initial LIDT in UV light. Then two batches of three samples were prepared with two protocols summarized in Figs. 1 and 2.

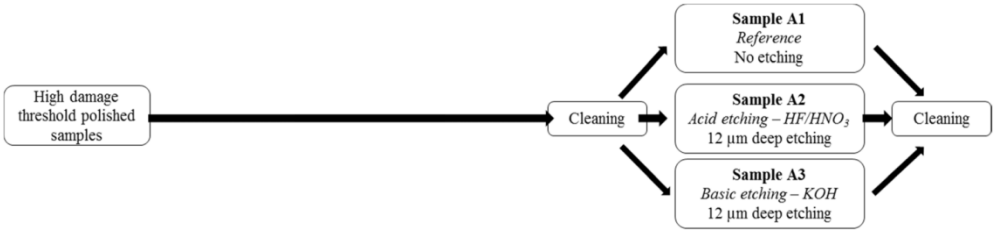

Fig. 1. Preparation of the samples for surface characterizations

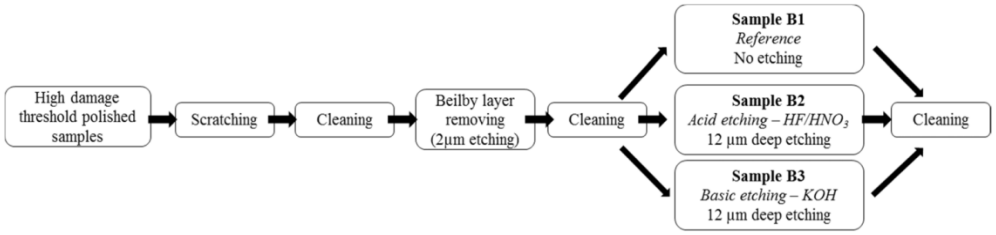

Fig. 2. Scratched samples preparation

The first batch (named samples A1 to A3) is reserved for polished surface characterization whereas the second batch (named samples B1 to B3) concerns the characterization of scratches. So the second batch needed intermediate steps to make the scratches and to show them up. Scratches were created by polishing using a single side polishing machine (Logitech PM5). Polishing was 30 min long and the slurry was composed of cerium oxide particles in colloidal silica. To remove the polishing layer and reveal scratches, a light wet etching (2 µm deep) was performed on these samples with a mixture of hydrofluoric acid HF (2.7wt%) and nitric acid HNO_3 (22.8wt%) at room temperature and with the system presented in Fig. 3. The two batches of samples were cleaned in an automatic washing machine. The cycle started

Optics EXPRESS

with a washing using a basic detergent at 60°C, then a rinsing, a second washing using an acid detergent at 40°C and finished with several rinsing steps.

After cleaning, two samples A1 and B1 were not etched to be kept as references and for the other samples two types of etching were performed with an acid or a basic chemical solution. Etching rates were equivalent (25 nm/min) for samples A2 and A3.

Sample A2 and sample B2 were etched with a mixture of hydrofluoric acid HF (2.7wt%) and nitric acid HNO_3 (22.8wt%) at room temperature. Samples were placed on three PTFE shims then the chemical solution was injected under samples (Fig. 3). Solution was static under sample as long as necessary in order to remove the specified amount of material. This system etched only one side on the sample.

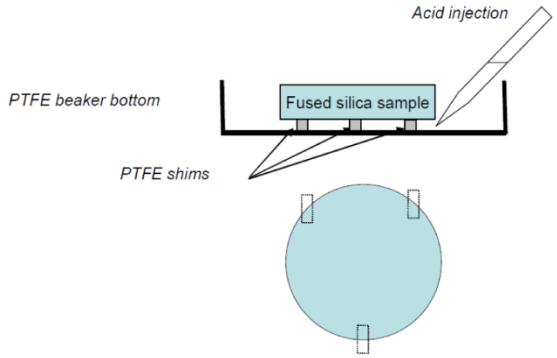

Fig. 3. Etching system used for the hydrofluoric solution (sample A2 and sample B2)

Sample A3 and sample B3 were placed in a beaker full of KOH solution (30wt%) heated at 100°C [30]. Figure 4 is an outline of this etching system. A magnetic stirrer shook the solution, consequently this system was dynamic and both sides of sample were etched.

Material removal after deep etching process was estimated by mass loss measurements.

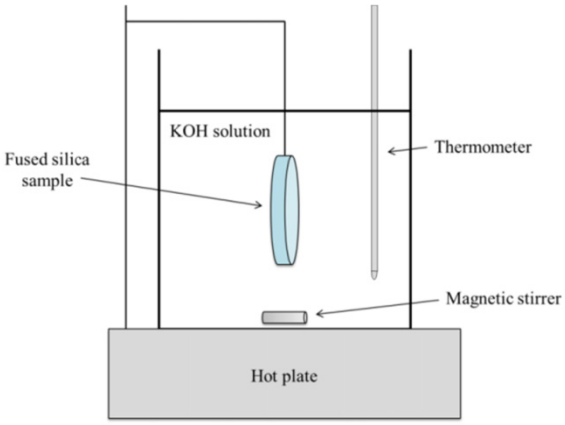

Fig. 4. Etching system for the KOH solution (Sample A3 and sample B3)

The layers removed by the deep etching were 12 µm deep. This value of 12 µm corresponds approximately to the inflection of the curve presented in Fig. 4 of reference [19] and so is an optimum value between the etched amount and the laser damage performance. Moreover minimizing the material removal of this deep etching is favorable to preserve the other optical performances.

Optics EXPRESS

2.2 Surface quality characterizations

Surface quality characterizations were performed on the etched polished surfaces (Samples A1, A2 and A3). Three techniques were used and repeated before and after deep etching.

To observe the whole sample surface and estimate the quantity of defects existing on the surface, we used a Defects Mapping System (DMS). DMS is composed of a LED ring placed around the sample and a high resolution camera. Surface defects scatter light coming from the LED and appear bright on a dark field [16].

An interferometer and an Atomic Force Microscope (AFM) were employed to measure roughness. The interferometer was a Zygo New View 7200 white light equipped with 1x, 10x and 100x objectives. The analysis areas were 10 mm x 10 mm, 1 mm x 1 mm, 100 µm x 100 µm respectively. AFM was a Bruker device used with scan asyst air tips and Peak Force tapping mode. Analysis area was 5 µm x 2.5 µm. The scan rate was 0.250 Hz with 512 samples/line and 250 pN for the peak force set point.

2.3 Surface chemical properties characterizations

Surface properties were studied on the deep etched polished surface (Samples A2 and A3). Surface free energy of fused silica was measured immediately after etching using a Drop Shape Analyzer DSA30 (Krüss). Drops of standard liquids (water, cyclohexane and ethylene glycol) were placed on sample surface then the wettability was measured for each liquid and then the surface free energy of sample was calculated.

We analyzed the superficial bonds with XPS measurements performed on a K-Alpha device (Thermofisher Scientific) using a monochromatic Al $K\alpha_{1,2}$ source (1486.6 eV) and a 400 µm spot diameter. Electronic charge compensation and an aluminum link have been performed because fused silica samples are insulating.

2.4 Laser damage testing

A Nd:YAG laser delivering a 355 nm wavelength and 3 ns pulse duration has been used. The beam had a Gaussian spatial profile with a diameter of 600 µm at 1/e. 10:1 damage test procedure (ISO 21254 [31]) was used. If no damage site appeared, the site was illuminated ten times at the maximum with a constant fluence and if a damage site was created, we stopped the 10 shots series. The laser fluence was measured simultaneously. Approximately 45 scratches were tested on each sample (Samples B1, B2 and B3). During the test, sample was illuminated with a white light coming from an optical fiber and scattered through a diffuser. This system was completed with a camera to detect the laser induced damage sites at video frequency.

3. Results

3.1 Set of samples A: etched surface

3.1.1 Surface quality characterizations

Defects Mapping System

Surface characterizations as obtained with the Defects Mapping System (DMS) are presented Fig. 5 using the same lighting and detection conditions. The bright points in the center and on the top of the samples are indents which have been deliberately made to be used as fiducials.

Optics EXPRESS

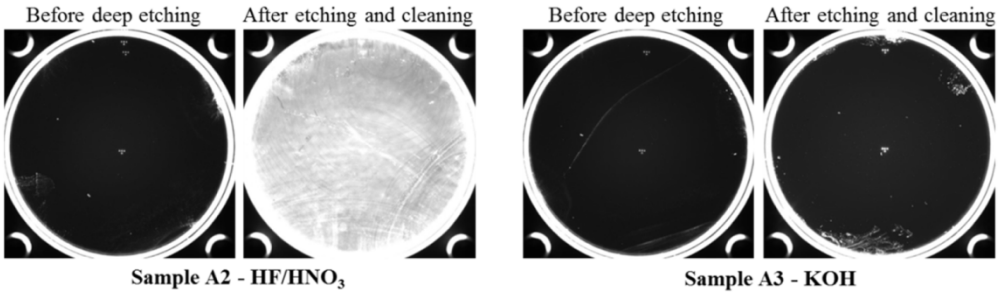

Fig. 5. DMS observations before and after deep etching of the whole surface of 50 mm diameter samples (Samples A2 and A3). Identical lighting and detection conditions. Bright spots in the center and on the top are fiducials.

Before etching, samples surfaces quality was equivalent and with very few localized scratches and digs. After etching, the surface treated with KOH did not really change whereas the one etched with HF/HNO_3 was totally transformed. On the KOH sample, some marks can be seen on top and bottom of the figure. We have been able to remove these white marks with a manual ethanol wiping. These marks have been therefore caused by the cleaning step after etching. Conversely, defects observed on the surface of the sample etched with HF/HNO_3 could not be removed by manual cleaning. Acid etching created a homogeneous scattering haze on the whole surface. However, this haze was difficult to observe without DMS or without high power lighting.

Roughness measurements

Roughness measurements were performed before and after deep etching with three objectives (1x, 10x and 100x). In order to achieve better statistics, measurements were carried out on three points located in the center, at the middle of the radius and at 5 mm from the edge. Means of root-mean squared roughness (RMS) are reported in Table 1. For roughness measurements, the size of the analysis area defines the spatial period of the defects we want to characterize. The 1x objective has a 10 mm x 10 mm analysis area and was appropriate to characterize defects with spatial periods ranging between 1 mm and 100 µm. The 10x objective has an analysis area ten times smaller and was used for analyzing spatial periods of defects ranging between 100 µm and 10 µm. Finally, the 100x objective was used for analyzing spatial periods of defects ranging between 10 µm and 1 µm.

Table 1. RMS roughness measurements (nm) on polished surface before and after deep etching.

	Objective Analysis area Spatial period	**1X** 10 mm x 10 mm [1mm ; 100µm]	**10X** 1 mm x 1 mm [100µm ; 10µm]	**100X** 100 µm x 100 µm [10µm ; 1µm]
Sample A2 - HF/HNO_3	Before etching	0.4 ± 0.06	0.2 ± 0.06	0.4 ± 0.07
	After etching	1.3 ± 0.06	1.2 ± 0.06	3.2 ± 0.07
Sample A3 – KOH	Before etching	0.4 ± 0.06	0.2 ± 0.06	0.4 ± 0.07
	After etching	0.3 ± 0.06	0.2 ± 0.06	0.2 ± 0.07

Before etching, RMS roughness measurements were equivalent for both samples. HF/HNO_3 etching degraded the surface quality and increased the roughness. This result is consistent with the DMS observations presented in Fig. 5. In contrast, the roughness values on the KOH etched surface were kept constant or barely reduced.

Optics EXPRESS

Atomic Force Microscopy

The highest magnification on the interferometer allowed us to analyze spatial periods between 10 µm and 1 µm. To improve the spatial resolution and observe smaller defects, we used an AFM. One measurement per sample was performed. Surface topographies mapping are presented in Fig. 6 with a unique vertical scale to compare the three measurements.

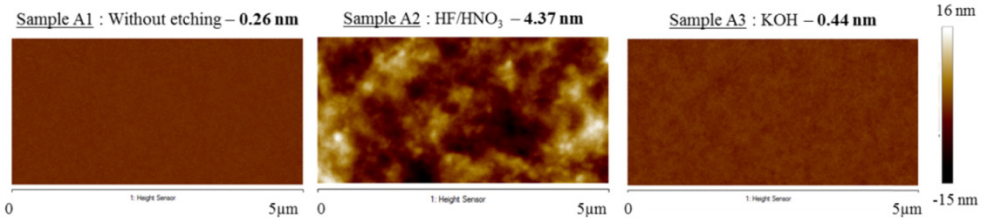

Fig. 6. AFM characterizations and roughness measurements (Samples A1, A2, and A3)

Surface quality was only slightly deteriorated after the basic etching compared to the "without etching" case. The RMS roughness measured on this micrometric area was doubled with this chemical treatment. At the opposite, the HF/HNO_3 solution strongly spoiled the sample surface quality; RMS roughness value was multiplied by twenty compared to the "without etching" case. Figure 7 represents the surface profiles obtained from these AFM measurements.

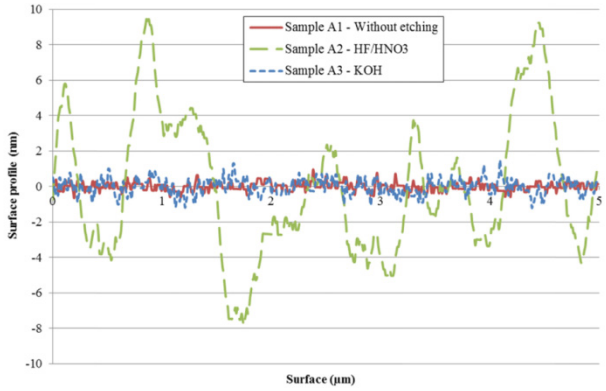

Fig. 7. Surface profiles obtained from the AFM measurements on the surfaces etched with HF/HNO_3 solution or KOH solution and on the polished surface without etching

Figure 7 confirms that surface profile is strongly modified after a HF/HNO_3 etching which is consistent with the large roughness increasing. These AFM measurements confirmed the DMS observations and interferometer roughness measurements which revealed surface quality deterioration with the HF/HNO_3 solution.

3.1.2 Surface chemical properties characterizations

Surface free energy measurements

Surface free energy measurements were performed immediately after etching. Surface treated by the HF/HNO_3 solution presented a surface free energy of 56 mN/m whereas one treated by the KOH solution was 64 mN/m. The surface free energy of a polished fused silica is around 30 mN/m, therefore the etching is an efficient method to improve the wettability of the fused silica surface especially with the use of a basic solution. A higher surface free energy corresponds to a better chemical affinity between the glass surface and liquids in contact.

Optics EXPRESS

X-Ray Photoelectron Spectroscopy

XPS characterizations were performed to identify the superficial bonds on the sample surfaces after etching and cleaning. Silicon, oxygen, carbon and sodium were detected. No species from the chemical etching solutions such as K or F were detected on the XPS spectra. Atomic quantification has been performed on each sample surface and results are summarized in Table 2. Sodium concentration detected on sample A3 is weak and close to the detection limit thus we considered it not significant. On the other hand, carbon concentrations were found to be relatively high for both samples with 4.4% for sample A2 and 7.7% for sample A3.

Table 2. XPS atomic quantification on etched surfaces. Measurements were done after etching and cleaning.

	Si	O	C	Na
Sample A2 – HF/HNO_3	36.2%	59.4%	4.4%	-
Sample A3 - KOH	34.3%	57.4%	7.7%	0.4%

Carbon high resolution XPS spectra have been performed to detail carbon links. Spectra obtained on both samples are presented Fig. 8.

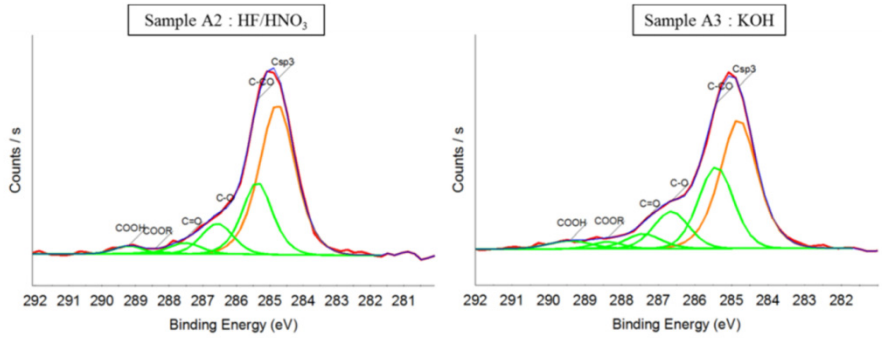

Fig. 8. Carbon high resolution XPS spectra obtained after cleaning on a sample etched with a HF/HNO_3 solution (Sample A2) and on a sample etched with a KOH solution (Sample A3)

Figure 8 evidences the presence of oxidized carbon bonds such as C-CO, C-O and C = O on both sample surfaces. A few carboxylic acid functions COOH and ester functions COOR had also been detected. Those carbon high resolution XPS spectra showed a higher content of oxidized carbon bonds on the surface after etching with KOH solution compared to the HF/HNO_3 solution.

3.2 Set of samples B: etched scratches

3.2.1 Scratches morphology characterizations

Defects mapping system

The quantity of scratches was evaluated with the DMS after their creation by polishing, after the Beilby layer removing (2µm etched) and after deep etching. Images are presented in Fig. 9 using the same lighting and detection conditions.

Optics EXPRESS

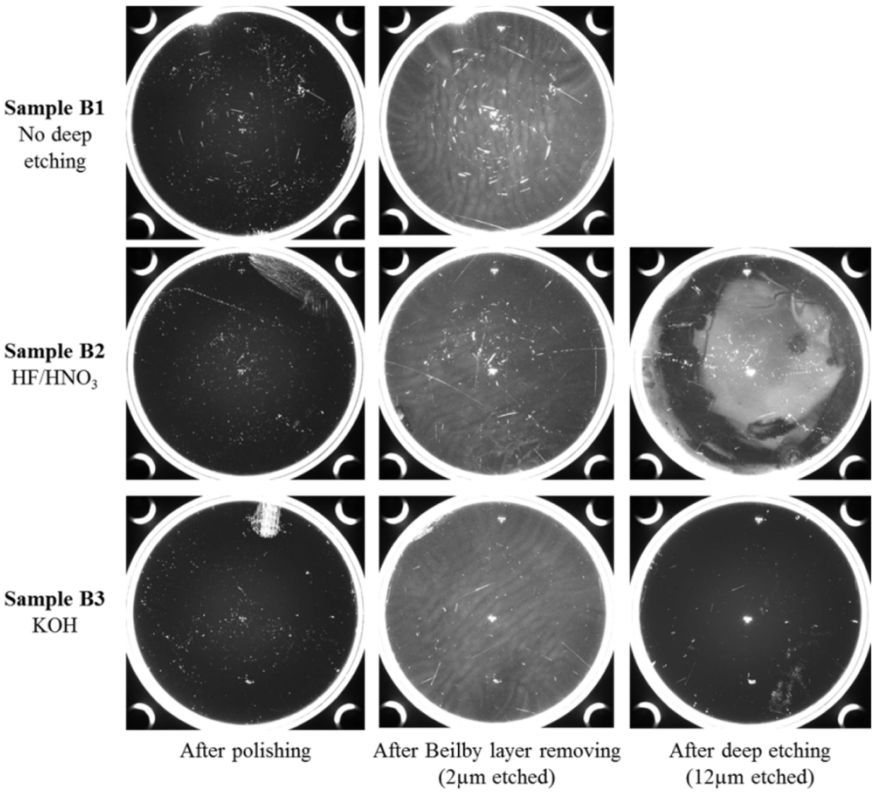

Fig. 9. DMS observations of scratched samples after polishing (left), Beilby layer removal (center) and deep etching (right). Bright spots in the center and on the top of the samples are indents which have been deliberately made to be used as fiducials. Bright points randomly distributed at the surface after polishing are due to a low quality of the cleaning performed after polishing.

The 2 µm light etching was necessary to reveal most scratches. Indeed most scratches created during our scratching process are embedded under the Beilby layer (a mix of cerium and colloidal silica is used). Therefore, the light wet etch is necessary to count and measure them. This 2 µm wet etch revealed also a discreet haze on all samples. The haze became worse after a deep etching performed with the HF/HNO_3 solution. Opposite, the KOH etching removed the haze and leaved the surface free of defects and perfectly transparent.

Optical microscope observations

Scratches morphology was studied with an optical microscope after the Beilby layer removing and after the deep etching for both sample B2 and B3. There is no noticeable morphology difference between HF/HNO_3 and KOH etching. The scratches exhibit the same width and aspect after HF/HNO_3 and KOH etching. Figure 10 presents the typical morphology observed on our samples. For the most part, scratches were brittles and continuous.

Optics EXPRESS

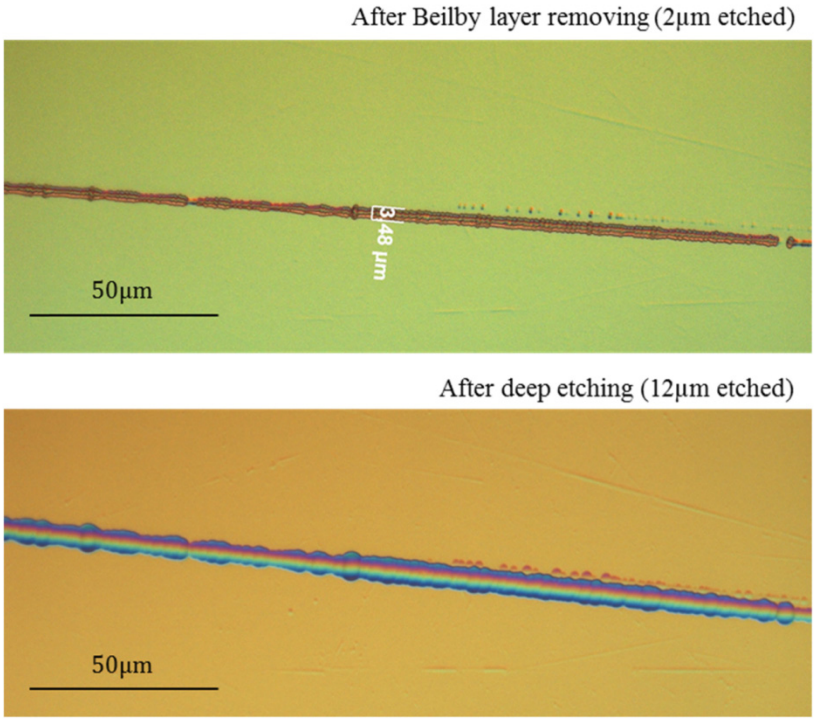

Fig. 10. Optical microscope observations of a scratch after 2µm etching (top) and a 12 µm deep etching (bottom)

The scratches widths were measured from these optical observations. About fifteen scratches were measured per samples. The Table 3 describes the mean and the range of the scratches widths after Beilby layer removing first and then after 12 µm deep etching for all the samples of batch B2 and B3.

Table 3. Scratches widths measurements (Batches B2 and B3).

	Minimum	Maximum	Mean
After Beilby layer removing	2 µm	8 µm	4 µm
After 12 µm deep etching	4 µm	16 µm	8 µm

3.2.2 Laser damage testing

Laser damage tests performed on the samples B1, B2 and B3 allow assessing the laser damage probability of scratches. The test protocol is described in the paragraph 2.4 and we used the data treatment explained by Jensen *et al.* [32] to calculate the probabilities. This data treatment assumes that an undamaged test site would have also survived when irradiated at lower fluence and a damaged test site would have also been damaged when irradiated at higher fluence. This way to treat data allows to take into account a data point in several data groups and consequently to virtually increase the available amount of data. Error on the probability was calculated with the formula $P((1-P)/(N*P))^{1/2}$ with P the probability and N the amount of irradiated sites.

Laser damage probability of etched scratches is presented on Fig. 11.

Optics EXPRESS

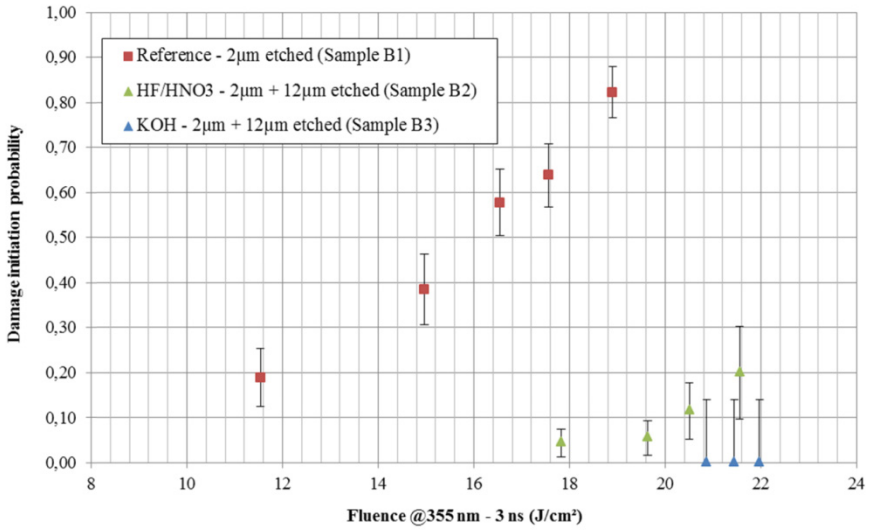

Fig. 11. Laser damage probability versus laser fluence at 355 nm and 3 ns for the scratched and etched samples (B1: red squares – reference, B2: green triangles – HF/HNO_3 etching, B3: blue diamonds – KOH etching).

The laser damage resistance of the scratches is highly improved after deep etching, whatever the etching solution. No damage site was created on the scratches etched with the basic solution consequently probabilities represented by blue triangles are null. In this case, the error bar is incalculable and fixed at 14%. Only three damage sites appeared on the scratches etched with the acid solution, over a total of 46 irradiated sites. Probabilities represented in Fig. 11 (green diamonds) were calculated from these three damage sites with the data treatment explained previously. However, because of the small proportion of initiated damage sites, it is hazardous to conclude that the laser damage performances of scratches etched with the KOH solution are better

Figure 11 shows that the LIDT of scratches is also around 20 J/cm^2. Laser damage tests were also performed on surfaces without defects etched with the same chemical solutions and conditions. These tests revealed neither improvement nor deterioration of the laser damage resistance of surface after deep etching. Moreover, the LIDT of surface was around 20 J/cm^2. We conclude that deep etching as no impact on the LIDT of surface without defects but it is an efficient technique to passivate the scratches.

4. Discussion

The deep etching considerably improved the laser induced damage threshold of scratches. Their LIDT was limited by the LIDT of the substrate and this effect was obtained with both chemical solutions. This large improvement of the LIDT of scratches due to the etching was also observed in previous studies with the BOE solution. In 2010, Suratwala *et al.* [19] proved that the deeper the etching, the higher the LIDT of scratches (which were manufactured with a unidirectional polishing protocol). In 2015, Wang *et al.* [33] increased the LIDT of scratches from 5 J/cm^2 to 12 J/cm^2 in UV light and nanosecond pulse laser thanks to a 20 µm deep etching using a similar BOE wet etching solution. Wang's scratches were generated by sliding a sphere indenter against fused silica surface. These studies revealed that etching had beneficial impacts on several scratches morphologies. In our case, LIDT improvement of scratches was also observed. Moreover, we demonstrated that the etching with KOH solutions lead to similar benefits on laser damage resistance of scratches. A previous study [34] revealed that the polishing induced contamination is detected until 1 µm deep in scratches thus a deep etching totally removed contamination from scratches. The LIDT improvement of

Optics EXPRESS

scratches after deep etching is therefore likely to be due to their morphology changes and also due to the reduction of the amount of sub-band gap absorbing defects. Actually, scratches morphology modifications with etching could reduce the electromagnetic field enhancement in the vicinity of the scratch [10]. These effects have to be studied in more details.

Different solutions (HF/HNO_3, BOE, KOH solutions) and devices can be used to obtain high laser damage resistance on scratches after deep etching but all these solutions and devices do not have the same effect on surface quality which is also a very important point for ICF optics. Etching of silica plates with a HF/HNO_3 solution strongly deteriorated their surface quality creating a scattering haze on the whole sample surface and highly increasing roughness. At the opposite, deep etching with a KOH solution modified neither the surface appearance nor the surface roughness while the etching removal rates and depths were equivalent with the two solutions. The XPS measurements performed after etching and cleaning did not evidence chemical differences between samples surfaces treated with HF/HNO_3 or KOH solutions. So it seems to us that the nature of the haze is topologic and not chemical. The surface quality degradation and the roughness increasing obtained with HF/HNO_3 solution were also reported in previous studies. For example, Wang *et al.* [33] measured a RMS surface roughness after a 20 µm deep HF etching from 3 nm to up to 50 nm in some cases whereas the initial surface roughness was <1 nm (analysis area 270 µm x 353 µm). With the same etching depth, Xu *et al.* [35] reported roughness deterioration from 0.6 nm to 0.9 nm (analysis area 640 µm x 480 µm). This roughness increase observed by Wang *et al.* and Xu *et al.* was attributed to the development of digs less than 1 µm deep after deep etching associated to prior grinding and polishing steps. It evidences that initial quality of the grinding and polishing processes prior etching is crucial for the final surface roughness after etching. Despite the fact that our roughness results obtained with the 100x objective on the HF/HNO_3 etched sample (sample A2) are consistent with Wang *et al.* data, grinding and polishing cannot be responsible for this effect. Hence, our since surface after etching is free of residual digs or specific features associated with grinding or polishing machine cinematics and/or abrasives. In contrast, the basic chemical treatment did not change the surface aspect and RMS roughness. It is important to notice that HF/HNO_3 etching was static whereas KOH etching was dynamic thanks to a magnetic stirrer. Furthermore, etching removal rates and the layer removed depths were equivalent with both solutions. Consequently, the surface quality degradation and the roughness elevation on the sample etched with HF/HNO_3 can be due to nature of the chemical solutions and/or to the etching experimental systems. In the case of a static etching, the dissolved silica is not dispersed into the solution subsequently the bath is no longer homogeneous and the removal rate can change at microscale. This could be an explanation of the better results obtained on the surface quality with the basic treatment. Surface reactivity was analyzed with surface free energy measurements. The surface free energy measurements were performed immediately after etching and revealed that the surface etched with a KOH solution had a higher surface free energy than the surface etched with the acid solution. A higher surface free energy promotes the interactions between the surface and liquids. Due to this improved interaction, this result is also in favor of a higher effectiveness for the alkaline treatment compared to the acidic one.

5. Conclusions

We tested KOH solution as an alternative to HF solution for deep etching operation on fused silica optics. KOH solution gave results as good as HF solution for laser damage resistance on fused silica optics, especially on scratches which are the weak points of UV optics. But there is a significance difference between both solutions in the experimental conditions we compared: surface quality, in term of roughness and aspect, is not deteriorated by KOH solution contrary to HF solution. The surface free energy results and XPS measurements lead us to believe that this surface morphology differences may be due to surface reactivity but complementary analysis is needed to understand more precisely the chemical reaction.

Optics EXPRESS

Finally, considering that higher safety conditions can be achieved when using OH based solutions compared to the use of HF based solutions, we believe that OH deep wet etching is a promising technique for the manufacturing of fused silica UV optics of high power laser facilities [30].

Acknowledgments

We would like to gratefully acknowledge the help of Laurent Lamaignère and Thierry Donval for laser damage testing. We acknowledge also Carole Houée for the large number of observations and characterizations she had performed.